Challenges for MSSM Higgs boson searches at hadron colliders

M. Carena,[1] A. Menon,[2,3] and C. E. M. Wagner[2,3,4]

[1]*Theoretical Physics Department, Fermi National Laboratory, Batavia, Illinois 60510, USA*
[2]*HEP Division, Argonne National Laboratory, 9700 Cass Ave., Argonne, Illinois 60439, USA*
[3]*Enrico Fermi Institute, University of Chicago, 5640 S. Ellis Ave., Chicago, Illinois 60637, USA*
[4]*KICP and Department of Physics, University of Chicago, 5640 S. Ellis Ave., Chicago, Illinois 60637, USA*

(Received 26 April 2007; published 15 August 2007)

In this article we analyze the impact of B physics and Higgs physics at LEP on standard and nonstandard Higgs bosons searches at the Tevatron and the LHC, within the framework of minimal flavor violating supersymmetric models. The B-physics constraints we consider come from the experimental measurements of the rare B decays $b \to s\gamma$ and $B_u \to \tau\nu$ and the experimental limit on the $B_s \to \mu^+\mu^-$ branching ratio. We show that these constraints are severe for large values of the trilinear soft breaking parameter A_t, rendering the nonstandard Higgs searches at hadron colliders less promising. On the contrary these bounds are relaxed for small values of A_t and large values of the Higgsino mass parameter μ, enhancing the prospects for the direct detection of nonstandard Higgs bosons at both colliders. We also consider the available ATLAS and CMS projected sensitivities in the standard model Higgs search channels, and we discuss the LHC's ability in probing the whole MSSM parameter space. In addition we also consider the expected Tevatron collider sensitivities in the standard model Higgs $h \to b\bar{b}$ channel to show that it may be able to find 3σ evidence in the B-physics allowed regions for small or moderate values of the stop mixing parameter.

DOI: 10.1103/PhysRevD.76.035004 PACS numbers: 12.60.Jv

I. INTRODUCTION

Over the last 20 years, the standard model (SM) has provided an exceptionally accurate description of all high energy physics experiments—whether they be electroweak precision or flavor physics observables. The only part of the standard model that remains to be tested is the mechanism for electroweak symmetry breaking. In the standard model, electroweak symmetry breaking is achieved by the scalar Higgs field acquiring a vacuum expectation value (vev), thereby giving mass to the quarks, leptons, and gauge bosons. However, this mechanism for electroweak symmetry breaking has a problem in that the Higgs potential is unstable with respect to radiative corrections, that is the scalar Higgs mass gets radiative corrections proportional to the cutoff due to fermion and boson loops. A number of extensions of the standard model have been suggested to try to alleviate this problem. Supersymmetry is one of the most promising of these extensions of the SM, in which every SM fermion (boson) has a spin-0 (spin-1/2) superpartner.

The minimal supersymmetric extension of the standard model or MSSM, with gauge invariant SUSY breaking masses of the order of 1 TeV, predicts an extended Higgs sector with a light SM-like Higgs boson of mass lower than about 130 GeV [1–12] that is in good agreement with precision electroweak measurements. However the flavor structure of these SUSY breaking masses is not well understood. If there are no tree-level flavor changing neutral currents associated with the gauge and supergauge interactions, the deviations from SM predictions are small. Such small deviations can be achieved if the quark and squark mass matrices are block diagonalizable in the same basis (an example is flavor blind squark and slepton masses). The flavor violating effects in these minimal flavor violating models are induced by loop factors proportional to Cabibbo-Kobayashi-Maskawa (CKM) matrix elements as in the standard model. The B-physics properties of these kinds of supersymmetric extensions of the SM have been studied in great detail in Refs. [13–20].

The recent improvements in our understanding of B-physics observables have put interesting constraints on Higgs searches in the minimal supersymmetric standard model (MSSM) at the Tevatron and LHC colliders. In Ref. [21] we analyzed the constraints that the nonobservation of the $B_s \to \mu^+\mu^-$ rare decay and the measurement of the $b \to s\gamma$ rare decay put on nonstandard model Higgs searches at hadron colliders. In this article, we additionally explore the regions of SUSY parameter space that can be probed in SM-like Higgs searches for different benchmark scenarios. We also extend our analysis in the B-physics sector to include the additional information coming from the recent measurement of $\mathcal{BR}(B_u \to \tau\nu)$ at Belle [22] and *BABAR* [23]. We find an interesting region of parameter space (i.e. large values of the Higgsino mass parameter μ and moderate values of the stop mixing parameter X_t) for which nonstandard Higgs searches are not strongly constrained by B physics. In particular, we find that scenarios with small stop mixing, like the so-called minimal mixing scenario [24], and large Higgsino parameter μ look very promising for the Tevatron and the LHC. B-physics constraints in these scenarios seem to allow the region around a CP-odd Higgs mass $M_A \sim 160$ GeV and $\tan\beta \sim 50$ (where $\tan\beta = v_2/v_1$ is the ratio of the two Higgs vev's), which can be easily probed at the Tevatron in the

near future. For nonstandard Higgs searches we show the present D0 [25] and CDF [26] excluded regions in the M_A-$\tan\beta$ plane with 1 fb^{-1} of data in the $\tau\tau$ inclusive channel and the Tevatron and LHC available projections for 4 fb^{-1} and 30 fb^{-1} [27,28], respectively, that depend only slightly on the other low energy SUSY parameters. Small to moderate MSSM Higgs masses are also interesting from the point of view of direct dark matter detection experiments, since in that case t-channel Higgs exchange contributes importantly to neutralino dark matter scattering off nuclei. This contribution implies a strong connection between the constraints on SUSY parameters from direct dark matter searches and nonstandard MSSM Higgs searches at colliders. In particular, the present direct detection limits on neutralino dark matter within the MSSM puts strong constraints on Higgs searches unless the Higgsino component of the neutralino is quite small (i.e. large values of μ), independent of the stop sector parameters [29].

This article is organized as follows. In Sec. II, we define our theoretical setup for both the B-physics constraints and Higgs searches within the MSSM. In Sec. III, we discuss representative benchmark scenarios that have different properties for B physics and Higgs searches. We show that within the MSSM there is a strong complementarity between the constraints coming from nonstandard Higgs searches and rare B decays. Taking into account these constraints we study the potential for standard model-like Higgs boson discovery at the Tevatron and the LHC [27,28]. For the Tevatron Higgs searches we assumed, conservatively, a final Tevatron luminosity of 4 fb^{-1}, while for Higgs searches at LHC, in the early phase, we used the expected 30 fb^{-1} luminosity estimates. Finally we conclude in Sec. IV.

II. THEORETICAL SETUP

A. Higgs searches and benchmark scenarios

1. Couplings and masses of the Higgs sector in the MSSM

In the MSSM there are three neutral scalar Higgs fields. Assuming no extra sources of CP violation in the MSSM beyond that of the SM, there are two CP-even Higgs bosons which are admixtures of the real neutral H_1^0 and H_2^0 components

$$\begin{pmatrix} h \\ H \end{pmatrix} = \begin{pmatrix} -\sin\alpha & \cos\alpha \\ \cos\alpha & \sin\alpha \end{pmatrix} \begin{pmatrix} H_1^0 \\ H_2^0 \end{pmatrix} \tag{1}$$

and an additional CP-odd Higgs field A, where α is the mixing angle that diagonalizes the CP-even Higgs mass matrix. The tree-level Higgs couplings to the SM fermions and gauge bosons are given by [30,31]

$$\begin{aligned} &\frac{1}{(\phi d\bar{d})_{\rm SM}((\phi u\bar{u})_{\rm SM})} \begin{pmatrix} (hd\bar{d})_{\rm MSSM}((hu\bar{u})_{\rm MSSM}) \\ (Hd\bar{d})_{\rm MSSM}((Hu\bar{u})_{\rm MSSM}) \\ (Ad\bar{d})_{\rm MSSM}((Au\bar{u})_{\rm MSSM}) \end{pmatrix} \\ &\quad = \begin{pmatrix} -\sin\alpha/\cos\beta(\cos\alpha/\sin\beta) \\ \cos\alpha/\cos\beta(\sin\alpha/\sin\beta) \\ \tan\beta(\cot\beta) \end{pmatrix}, \\ &\frac{1}{(\phi VV)_{\rm SM}} \begin{pmatrix} (hVV)_{\rm MSSM} \\ (HVV)_{\rm MSSM} \\ (AVV)_{\rm MSSM} \end{pmatrix} = \begin{pmatrix} \sin(\beta-\alpha) \\ \cos(\beta-\alpha) \\ 0 \end{pmatrix}, \end{aligned} \tag{2}$$

where V can be either the Z or W vector boson. At moderate or large values of $\tan\beta$, one of the two CP-even Higgs bosons tends to couple strongly to the gauge bosons while the other one only couples weakly. We will denote the Higgs boson that couples to the gauge bosons the strongest as SM-like. The CP-odd and the other CP-even Higgs bosons are denoted as nonstandard and have $\tan\beta$ enhanced couplings to the down quarks and leptons (see Eq. (2)).

The identification of the SM-like Higgs depends critically on the size of the pole mass of the pseudoscalar Higgs M_A. For large values of M_A, the lighter Higgs becomes SM-like and its mass has the approximate analytic form [1–3]

$$\begin{aligned} (M_h^{\rm max})^2 = M_Z^2\cos^2(2\beta)\left(1-\frac{3m_t^2}{8\pi^2 v^2}t\right) + \frac{3m_t^4}{4\pi^2 v^2}\left[\frac{1}{2}\tilde{X}_t + t \right. \\ \left. + \frac{1}{16\pi^2}\left(\frac{3m_t^2}{2v^2} - 32\pi\alpha_3\right)(\tilde{X}_t t + t^2)\right], \end{aligned} \tag{3}$$

where $\tilde{X}_t = \frac{2X_t^2}{M_{\rm SUSY}^2} - \frac{X_t^4}{6M_{\rm SUSY}^4}$, $X_t = A_t - \mu/\tan\beta$, $t = \log(\frac{M_{\rm SUSY}^2}{m_t^2})$, and $M_{\rm SUSY}$ is the geometric mean of the stop masses. In Eq. (3), we have included the leading two-loop radiative corrections from the stop sector but we have not included the two-loop corrections associated with the relation between the top quark mass and the top Yukawa coupling at the stop mass scale, that depends on the relative sign of the gluino mass and X_t [6]. At values of the CP-odd Higgs boson mass M_A less than $m_h^{\rm max}$ and large values of $\tan\beta$, $\alpha \sim \beta$ and the heavier CP-even Higgs is SM-like with mass given approximately by Eq. (3).

2. SM-like Higgs boson searches

The CMS and ATLAS collaborations have calculated the signal significance curves for standard model Higgs detection at the LHC. Because of the modified Higgs couplings in the MSSM, for the same Higgs masses, these estimates can change significantly with changes in the supersymmetric mass parameters. To quantify when the significance will be either enhanced or reduced we consider the quantity [30,31]

$$R = \frac{\sigma(P\bar{P}\to X\phi)_{\rm MSSM}\mathcal{BR}(\phi\to Y)_{\rm MSSM}}{\sigma(P\bar{P}\to X\phi)_{\rm SM}\mathcal{BR}(\phi\to Y)_{\rm SM}}, \tag{4}$$

where X are particles produced in association with the Higgs and Y are SM decay products of the Higgs.[1] As the predicted SM-like Higgs mass range within the MSSM is less than or about 130 GeV, we only consider the light Higgs production and decay channels $q\bar{q}\phi \to q\bar{q}\tau\bar{\tau}$ and $\phi \to \gamma\gamma$ at the LHC and $W/Z\phi(\phi \to b\bar{b})$ at the Tevatron. At a luminosity larger than 30 fb^{-1} at the LHC, the $t\bar{t}\phi$ will become effective. However as we are considering only the early phase of the LHC we will not study this process.

For the $q\bar{q}\phi \to q\bar{q}\tau\bar{\tau}$ channel the Higgs is produced dominantly by weak-boson fusion. Hence, the tree-level production cross section is proportional to the square of the $(\phi VV)_{\rm SM}$ coupling in Eq. (2), which implies that the ratio of production cross sections in Eq. (4) is proportional to $\sin^2(\beta-\alpha)(\cos^2(\beta-\alpha))$ when M_A is larger (smaller) than $M_h^{\rm max}$. At large $\tan\beta$ and $M_A > M_h^{\rm max}$ ($M_A < M_h^{\rm max}$) the Higgs mixing angle $\sin\alpha \sim -1/\tan\beta$ ($\cos\alpha \sim 1/\tan\beta$). Hence, in this region of the M_A-$\tan\beta$ plane the $(hVV)_{\rm MSSM}$ ($(HVV)_{\rm MSSM}$) couplings are very close to their SM values. Therefore at large $\tan\beta$ and small or large values of M_A, compared to $M_h^{\rm max}$, the ratio $\sigma(P\bar{P} \to X\phi)_{\rm MSSM}/\sigma(P\bar{P} \to X\phi)_{\rm SM}$ is close to 1. For $\phi \to \gamma\gamma$ channel the Higgs is mainly produced through gluon fusion which is induced by third generation quark and squark loops. For squark masses greater than 500 GeV, like those we are considering in this paper, the squark contributions are small and the SM-like Higgs has a production cross section similar to that of the standard model Higgs.

Whenever M_A is comparable to the SM-like Higgs mass, $|M_A - m_h^{\rm max}| \lesssim 10$ GeV, both the CP-even Higgs bosons acquire similar masses and have nonstandard gauge and Yukawa couplings. Hence for each of these channels we follow the prescription given in Ref. [30] and sum the contributions from both the CP-even Higgs states so that

$$R = \frac{\sigma(P\bar{P} \to Xh)_{\rm MSSM}\mathcal{BR}(h \to Y)_{\rm MSSM} + \sigma(P\bar{P} \to XH)_{\rm MSSM}\mathcal{BR}(H \to Y)_{\rm MSSM}}{\sigma(P\bar{P} \to X\phi)_{\rm SM}\mathcal{BR}(\phi \to Y)_{\rm SM}}, \tag{5}$$

because we assume that the two signals cannot be separated.

If M_A is larger (smaller) than $M_h^{\rm max}$ and the loop corrections to the off-diagonal elements of the CP-even Higgs mass matrix are small, then the large $\tan\beta$ induced corrections do not enhance or reduce the $hb\bar{b}$ ($Hb\bar{b}$) or $h\tau\bar{\tau}$ ($H\tau\bar{\tau}$) couplings and they remain standard model-like. Hence, in these regions of parameter space the branching ratios into either b's or τ's are close to their standard model values. The $\phi\gamma\gamma$ coupling is induced through quark loops and hence is generally small. However, in scenarios where the $\phi b\bar{b}$ and $\phi\tau\bar{\tau}$ couplings are suppressed, like, for example, if there is a cancellation of the off-diagonal CP-even mass Higgs matrix element due to radiative effects, the $\phi \to \gamma\gamma$ branching ratio can be relatively enhanced. We shall discuss this case in Sec. III C.

3. Nonstandard Higgs boson searches

At large $\tan\beta$ the nonstandard Higgs bosons are produced in association with bottom quarks or through gluon fusion. For both of these processes, at large $\tan\beta$, the relevant coupling is the bottom Yukawa coupling [24,32]. Therefore including the relevant large $\tan\beta$ radiative correction we find the production cross section is proportional to the square of the bottom Yukawa $y_b^2 = (y_b^{\rm SM})^2\tan^2\beta/(1+\epsilon_3\tan\beta)^2$, where the precise definition of this loop induced correction is given in Eq. (15). In addition, at large $\tan\beta$ [24,32] the branching ratio of the decay of the nonstandard Higgs boson into $\tau\tau$ is approximately given by

$$\mathrm{Br}(A, H \to \tau^+\tau^-) \simeq \frac{(1+\epsilon_3\tan\beta)^2}{(1+\epsilon_3\tan\beta)^2+9}. \tag{6}$$

Hence the total production rate of the CP-odd Higgs boson at large $\tan\beta$ is

$$\sigma(gg, b\bar{b} \to A) \times \mathcal{BR}(A \to \tau^+\tau^-) \sim \sigma(gg, b\bar{b} \to A)_{\rm SM}\frac{\tan^2\beta}{(1+\epsilon_3\tan\beta)^2+9}. \tag{7}$$

Therefore we can define a ratio similar to Eq. (4)

$$r = \frac{\sigma(gg, b\bar{b} \to A)_{\rm MSSM}\mathcal{BR}(A \to \tau^+\tau^-)_{\rm MSSM}}{\sigma(gg, b\bar{b} \to \phi)_{\rm SM}\mathcal{BR}(\phi \to \tau^+\tau^-)_{\rm SM}} \sim \frac{\tan^2\beta}{(1+\epsilon_3\tan\beta)^2+9} \tag{8}$$

and a analogous expression holds for the CP-even nonstandard Higgs boson production and decay rates.

B. B-physics observables and limits

We will consider the four B-physics observables: $\mathcal{BR}(B_s \to \mu^+\mu^-)$, ΔM_s, $\mathcal{BR}(b \to s\gamma)$, and $\mathcal{BR}(B_u \to \tau\nu)$ within the minimal flavor violating MSSM.

1. $\mathcal{BR}(B_s \to \mu^+\mu^-)$

In the standard model the relevant contribution to the $B_s \to \mu^+\mu^-$ process comes through the Z-penguin and the W-box diagrams which have the analytic form [18,33]

[1]For the region of parameter space we study only standard model decays are open.

$$\mathcal{BR}(B_s \to \mu^+\mu^-)_{\rm SM} = \frac{G_F^2\alpha_{\rm em}^2}{16\pi^3} M_{B_s}\tau_{B_s}F_{B_s}^2|V_{tb}V_{ts}|^2 \times\sqrt{1-\frac{4m_\mu^2}{M_{B_s}^2}}m_\mu^2 C_{10}^2(x_t), \quad (9)$$

where τ_{B_s} is the mean lifetime, F_{B_s} is the decay constant of the B_s meson, $x_t = m_t/M_W$, and

$$C_{10}(x) = b_0(x) - c_0(x), \quad (10)$$

$$c_0(x) = \frac{x}{8}\left[\frac{x-6}{x-1} + \frac{3x+2}{(x-1)^2}\ln(x)\right], \quad (11)$$

$$b_0(x) = \frac{1}{4}\left[\frac{x}{1-x} + \frac{x}{(x-1)^2}\ln(x)\right]. \quad (12)$$

Therefore the predicted SM value comes out to be [18,33]

$$\mathcal{B}\mathcal{R}(B_s \to \mu^+\mu^-)_{\rm SM} = (3.8 \pm 0.1)\times 10^{-9}. \quad (13)$$

However in the presence of supersymmetry at large $\tan\beta$, there are significant contributions from Higgs mediated neutral currents, which have the form [15,16]

$$\mathcal{BR}(B_s \to \mu^+\mu^-) = 3.5\times 10^{-5}\left[\frac{\tan\beta}{50}\right]^6\left[\frac{\tau_{B_s}}{1.5\ \text{ps}}\right] \times\left[\frac{F_{B_s}}{230\ \text{MeV}}\right]^2\left[\frac{|V_{ts}|}{0.040}\right]^2\frac{m_t^4}{M_A^4} \times\frac{(16\pi^2\epsilon_Y)^2}{(1+\epsilon_3\tan\beta)^2(1+\epsilon_0\tan\beta)^2}, \quad (14)$$

where

$$\epsilon_3 = \epsilon_0 + y_t^2\epsilon_Y. \quad (15)$$

The gluino loop factor ϵ_0 and the chargino-stop loop factor ϵ_Y are given by

$$\epsilon_0 \approx \frac{2\alpha_s}{3\pi} M_3\mu C_0(m_{\tilde{b}_1}^2, m_{\tilde{b}_2}^2, M_3^2), \quad (16)$$

$$\epsilon_Y \approx \frac{1}{16\pi^2} A_t\mu C_0(m_{\tilde{t}_1}^2, m_{\tilde{t}_2}^2, \mu^2), \quad (17)$$

respectively, where $m_{\tilde{b}_i}$ is the ith sbottom mass, $m_{\tilde{t}_i}$ is the ith stop mass, M_3 is the gluino mass, μ is the Higgsino mass parameter, A_t is the soft SUSY breaking stop trilinear parameter, and

$$C_0(x,y,z) = \frac{y}{(x-y)(z-y)}\log(y/x) + \frac{z}{(x-z)(y-z)}\log(z/x). \quad (18)$$

The present experimental exclusion limit at 95% C.L. from CDF [34] is

$$\mathcal{B}\mathcal{R}(B_s \to \mu^+\mu^-) \le 1\times 10^{-7}, \quad (19)$$

which puts strong restrictions on possible flavor changing neutral currents in the MSSM at large $\tan\beta$. Additionally, if no signal is observed, the projected exclusion limit, at 95% C.L., on this process for 4 fb^{-1} at the Tevatron is [27]

$$\mathcal{B}\mathcal{R}(B_s \to \mu^+\mu^-) \le 2.8\times 10^{-8}. \quad (20)$$

Similarly, if no signal is observed at the LHC, the projected ATLAS bound at 10 fb^{-1} is [35]

$$\mathcal{B}\mathcal{R}(B_s \to \mu^+\mu^-) \le 5.5\times 10^{-9}. \quad (21)$$

Therefore considering Eq. (14) in the absence of a signal, these experiments will put very strong constraints on the allowed MSSM parameter space. In addition, LHCb has the potential to claim a 3σ (5σ) evidence (discovery) of a standard model signature with as little as $\sim$2 fb^{-1} (6 fb^{-1}) of data [36].

2. ΔM_s

In the standard model the dominant contribution to ΔM_s comes from W-top box diagrams that have the analytical form [15,16]

$$\Delta M_s = \frac{G_F^2 M_W^2}{6\pi^2} M_{B_s}\eta_2 F_{B_s}^2\hat{B}_{B_s}|V_{ts}|^2 S_0(m_t), \quad (22)$$

where M_{B_s} is the B_s meson mass, $\hat{B}_{B_s}$ is the B_s bag parameter, η_2 is the NLO QCD factor, and

$$S_0(m_t) \simeq 2.39\left(\frac{m_t}{167\ \text{GeV}}\right)^{1.52}. \quad (23)$$

The updated theoretical predictions from the CKMfitter and UTFit groups are slightly different. The UTFit group finds the 95% C.L. range [37]

$$(\Delta M_s)^{\rm SM} = (20.9 \pm 2.6)\ \text{ps}^{-1} \quad (24)$$

which is consistent with the CKMfitter groups' 2σ range [38]

$$13.4\ \text{ps}^{-1} \le (\Delta M_s)^{\rm SM} \le 31.1\ \text{ps}^{-1} \quad (25)$$

and central value of 18.9 ps^{-1}.

About a year ago, the D0 collaboration reported a signal consistent with values of ΔM_s in the range

$$21\ (\text{ps})^{-1} > \Delta M_s > 17\ \text{ps}^{-1} \quad (26)$$

at the 90% C.L. [39]. More recently, the CDF collaboration has made a measurement, with the result [40]

$$\Delta M_s = (17.77 \pm 0.10(\text{stat}) \pm 0.07(\text{syst}))\ \text{ps}^{-1}. \quad (27)$$

The large theoretical uncertainties and the precise experimental value suggest that small or moderate negative contributions to ΔM_s may be easily accommodated. As shown in Refs. [14–16,18] for large $\tan\beta$ and uniform squark masses one obtains negative contributions to ΔM_s

that are well approximated by

$$(\Delta M_s)^{\rm DP} = -12.0\ {\rm ps}^{-1}\left[\frac{\tan\beta}{50}\right]^4\left[\frac{F_{B_s}}{230\ {\rm MeV}}\right]^2\left[\frac{V_{ts}}{0.04}\right]^2 \times \left[\frac{\bar{m}_b(\mu_s)}{3.0\ {\rm GeV}}\right]\left[\frac{\bar{m}_s(\mu_s)}{0.06\ {\rm GeV}}\right]\left[\frac{\bar{m}_t^4(\mu_s)}{M_W^2 M_A^2}\right] \times \frac{(16\pi^2\epsilon_Y^2)^2}{(1+\epsilon_3\tan\beta)^2(1+\epsilon_0\tan\beta)}. \quad (28)$$

In the next section we will discuss the interplay between the $\mathcal{BR}(B_s \to \mu^+\mu^-)$ in Eq. (14) and ΔM_s in Eq. (28) within the framework of minimal flavor violating MSSM.

3. $\mathcal{BR}(b \to s\gamma)$

The next B-physics process of interest is the rare decay $b \to s\gamma$. The world experimental average of the branching of this rare decay is [41,42]

$$\mathcal{BR}(b \to s\gamma)^{\rm exp} = (3.55 \pm 0.24^{+0.09}_{-0.10} \pm 0.03) \times 10^{-4}. \quad (29)$$

This experimental result is close to the SM central value and so puts constraints on flavor violation in any extension of the standard model. However, the theoretical uncertainties in the standard model for this process are quite large [42]

$$\mathcal{BR}(b \to s\gamma)^{\rm SM} = (2.98 \pm 0.26) \times 10^{-4}. \quad (30)$$

Using the experimental and SM ranges for the $\mathcal{BR}(b \to s\gamma)$ we find the 2σ allowed range is

$$0.92 \le \frac{\mathcal{BR}(b \to s\gamma)^{\rm MSSM}}{\mathcal{BR}(b \to s\gamma)^{\rm SM}} \le 1.46. \quad (31)$$

This bound is appropriate for constraining new physics contributions due to the cancellation of the dominant uncertainties coming from infrared physics effects.

In minimal flavor violating MSSM there are two new contributions from the charged Higgs and the chargino-stops diagrams. The charged Higgs amplitude, including the stop induced two-loop effects, is proportional to the factor [43,44]

$$A_{H^+} \propto \left[\frac{1 - \frac{2\alpha_s}{3\pi}\mu M_3 \tan\beta(\cos^2\theta_{\tilde{t}} C_0(m^2_{\tilde{s}_L}, m^2_{\tilde{t}_1}, M_3^2) + \sin^2\theta_{\tilde{t}} C_0(m^2_{\tilde{s}_L}, m^2_{\tilde{t}_2}, M_3^2))}{1+\epsilon_3\tan\beta}\right]\frac{m_t^2}{m_H^{+2}}, \quad (32)$$

where $\theta_{\tilde{t}}$ is the stop mixing angle. The chargino-stop amplitude has the form [43,44]

$$A_{\chi^-} \propto \frac{\mu A_t \tan\beta}{1+\epsilon_3\tan\beta} f(m^2_{\tilde{t}_1}, m^2_{\tilde{t}_2}, m^2_{\tilde{\chi}^-}), \quad (33)$$

where $f(m^2_{\tilde{t}_1}, m^2_{\tilde{t}_2}, m_{\tilde{\chi}^-}) \sim 1/\max(m^2_{\tilde{t}_1}, m^2_{\tilde{t}_2})$ is the one-loop factor that depends on the stop masses and the chargino mass. The specific dependences of these amplitudes on MSSM parameters are important in understanding the constraints on the SUSY contributions to $\mathcal{BR}(b \to s\gamma)$, which will be discussed below.

4. $\mathcal{BR}(B_u \to \tau\nu)$

The final B-physics observable of interest is the process $B_u \to \tau\nu$ which the Belle experimental collaboration finds to be [22]

$$\mathcal{BR}(B_u \to \tau\nu)^{\rm Belle} = (1.79^{+0.56}_{-0.49}({\rm stat})^{+0.46}_{-0.51}({\rm syst})) \times 10^{-4}, \quad (34)$$

while the *BABAR* collaboration finds a value [23]

$$\mathcal{BR}(B_u \to \tau\nu)^{BABAR} = (0.88^{+0.68}_{-0.67}({\rm stat}) \pm 0.11({\rm syst})) \times 10^{-4}. \quad (35)$$

The two values are within 2σ of each other and both of them are consistent with the standard model prediction. The average of these two experiments is [37]

$$\mathcal{BR}(B_u \to \tau\nu)^{\rm exp} = (1.31 \pm 0.48) \times 10^{-4}. \quad (36)$$

The standard model contribution is mediated by the W-boson and has the generic form [45]

$$\mathcal{BR}(B_u \to \tau\nu)^{\rm SM} = \frac{G_F^2 m_B m_\tau^2}{8\pi}\left(1 - \frac{m_\tau^2}{m_B^2}\right)^2 F_B^2 |V_{ub}|^2 \tau_B \quad (37)$$

and using the UTFit fitted value for $|V_{ub}| = (3.68 \pm 0.14) \times 10^{-3}$ (which is also in good agreement with the CKMfitter value [38]), τ_B, and the extracted value of $F_B = 0.237 \pm 0.037$ GeV leads to the value [37]

$$\mathcal{BR}(B_u \to \tau\nu)^{\rm SM} = (0.85 \pm 0.13) \times 10^{-4}. \quad (38)$$

Observe, however that the value of $|V_{ub}| = (4.49 \pm 0.33) \times 10^{-9}$, extracted from inclusive semileptonic decays is higher and leads to the standard model prediction $\mathcal{BR}(B_u \to \tau\nu)^{\rm SM} = (1.39 \pm 0.44) \times 10^{-4}$ [37].

In the MSSM there is an extra contribution due to the charged Higgs which interferes destructively with the SM contribution, so that at large $\tan\beta$ the ratio of the two is [45–47]

$$R_{B\tau\nu} = \frac{\mathcal{BR}(B_u \to \tau\nu)^{\rm MSSM}}{\mathcal{BR}(B_u \to \tau\nu)^{\rm SM}} = \left[1 - \left(\frac{m_B^2}{m_{H^\pm}^2}\right)\frac{\tan^2\beta}{1+\epsilon_0\tan\beta}\right]^2. \quad (39)$$

Now assuming a 2σ deviation in Eqs. (36) and (38) that is due to the charged Higgs contribution, we find the allowed range of values for this ratio to be

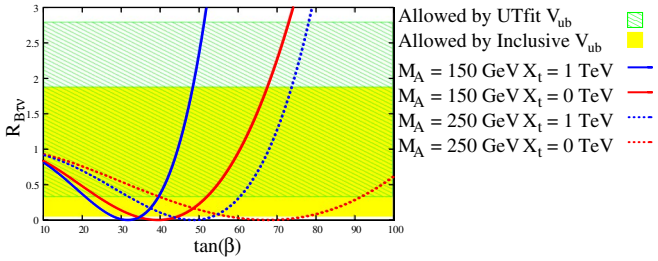

FIG. 1 (color online). The gray (green) hatched area is the 2σ allowed region of the ratio $R_{B\tau\nu}$ if the fitted value of $|V_{ub}|$ is used to calculate the standard model prediction of the $B_u \to \tau\nu$ decay rate. The light gray (yellow) is the corresponding region if the inclusive determination of $|V_{ub}|$ is used instead of the fitted value. The solid (dashed) lines show the variation of $R_{B\tau\nu}$ with respect to $\tan\beta$ for $M_A = 150$ GeV (250 GeV), while the gray (red) color and dark gray (blue) color correspond to $X_t = 0$ and $X_t = 1$ TeV, respectively.

$$0.32 \leq R_{B\tau\nu} \leq 2.77. \tag{40}$$

However as discussed above, if the inclusive determination of $|V_{ub}|$ is used instead of the fitted value we get a different range of allowed values for $R_{B\tau\nu}$. In Fig. 1 we show the effect of choosing the $|V_{ub}|$ inclusive value over the fitted value. The gray (green) hatched region is allowed if we use the fitted value of $|V_{ub}|$ while the light gray (yellow) region is allowed if we use the extracted value of $|V_{ub}|$ from inclusive semileptonic b decays. From Fig. 1 we can see that if $M_A = 150$ GeV and $X_t = 0$ the allowed values are $\tan\beta \sim 10$–25 and $\tan\beta \sim 53$–70 using the fitted value of $|V_{ub}|$, while using the inclusive value of $|V_{ub}|$ we find $10 \lesssim \tan\beta \lesssim 37$ or $43 \lesssim \tan\beta \lesssim 63$. Therefore, when we project this constraint onto the M_A-$\tan\beta$ plane the allowed regions are significantly different, especially at larger values of M_A. In particular the region of intermediate $\tan\beta$ that is excluded by the $B_u \to \tau\nu$ constraint is much smaller if we use the inclusive value of $|V_{ub}|$ instead of the fitted value because the lower bound on $R_{B\tau\nu}$ is smaller for the value extract from inclusive b decays. Whenever we consider the constraint on the $B_u \to \tau\nu$ rate in this paper we will use the fitted values, so expect our bounds to be quite conservative and one could enlarge the B-physics allowed region by going to larger values of $|V_{ub}|$.

III. B-PHYSICS CONSTRAINTS AND HIGGS SEARCHES AT HADRON COLLIDERS

In this section we shall use the above B-physics limits and Higgs search capabilities to put constraints on the allowed regions of MSSM parameter space. In particular we project these constraints onto the M_A-$\tan\beta$ plane. We also assume that all the squark masses are uniform and denoted by $M_{\rm SUSY}$, $2M_1 = M_2 = 500$ GeV and we use the central value for the top-quark measured, at the Tevatron, to be $m_t = 170.9 \pm 1.8$ GeV [48]. Within this framework we study four benchmark scenarios by varying the parameters μ, $X_t = A_t - \mu/\tan\beta$, $M_{\rm SUSY}$, and M_3. We numerically calculate the ratio r, defined for nonstandard Higgs searches in Eq. (8), using the CPsuperH program [49]. To estimate the present excluded region and the projected Tevatron reach we used the 1 fb^{-1} CDF results presented in Ref. [26], the projected 4 fb^{-1} curves from Ref. [27], and the 1 fb^{-1} D0 results from Ref. [25] for the maximal mixing scenario with $\mu \sim -200$ GeV. To estimate the LHC reach we used the results for the maximal mixing scenario with $\mu \sim -200$ GeV in Fig. 6 of Ref. [24], which is based on the study in Ref. [50]. Using Eq. (8), each of these curves are rescaled for each of the different parametric scenarios we consider in this paper. Let us stress that the results of Ref. [50] we are using, are in reasonably good agreement with the latest CMS studies for different τ decay final states, which include a full detector simulation [51–54].

For the SM-like Higgs searches at 30 fb^{-1}, we used the CMS and the ATLAS studies shown in Refs. [28,50] to estimate the signal significance in the $h \to \tau\tau$ and $h \to \gamma\gamma$ channel. We used CPsuperH [49] to calculate the relevant branching ratios and couplings needed to estimate the value of R in Eq. (4). For the Tevatron searches we used the updated values of the luminosity needed to discover a standard model Higgs, from Ref. [55], to estimate the variation of signal significance with respect to SM Higgs mass at 4 fb^{-1} for each experiment. The projections at the Tevatron assume an improvement in the sensitivity of detectors along with a basic increase in the luminosity [55].

Before presenting our analysis, let us stress that, from the form of the double penguin contribution to ΔM_s in Eq. (28) and the large $\tan\beta$ contribution to $\mathcal{BR}(B_s \to \mu^+\mu^-)$ in Eq. (14), it is clear that the two quantities are greatly correlated. As we have shown in Refs. [15,16] for the case of uniform squark masses, Eqs. (14) and (28) imply that

$$\frac{|(\Delta M_s)^{\rm SUSY}_{\rm DP}|}{\mathcal{BR}(B_s \to \mu^+\mu^-)_{\rm SUSY}} \sim \frac{0.034\ (\text{ps})^{-1}}{10^{-7}} \frac{M_A^2}{M_W^2} \left(\frac{50}{\tan\beta}\right)^2. \tag{41}$$

Notice that the only SUSY parameters this ratio depends on are M_A and $\tan\beta$. Considering the present experimental limit on $\mathcal{BR}(B_s \to \mu^+\mu^-)$ in Eq. (19), we showed in Ref. [21] that, as is apparent in Eq. (41), the double penguin contributions to ΔM_s can be at most a few ps^{-1} for $M_A < 1$ TeV. As these corrections are negative with respect to the SM contribution, they make the theoretical predictions agree slightly better with the experimentally measured value. However, given that the theoretical errors in Eqs. (24) and (25) are large and the SUSY contributions are small, the ΔM_s measurement only puts a very weak constraint on Higgs searches once the $B_s \to \mu^+\mu^-$ bound is imposed.

A. Large to moderate X_t and small μ

This scenario is a modified version of the one called maximal mixing because we chose the sign of $A_t M_3$ to be negative. This choice of sign tends to reduce the value of the SM-like Higgs mass making it easier for the Tevatron collider to possibly probe this scenario. On the other hand the change in the sign of M_3 with respect to that in the maximal mixing scenario [24] does not significantly affect B-physics constraints and the nonstandard Higgs boson search limits, as can be seen in Fig. 9(a) of Ref. [21]. The SM-like Higgs mass depends strongly on the stop mixing parameter X_t, and it attains its maximum value for $X_t \sim \sqrt{6} M_{\rm SUSY} = 2.4$ TeV. For these values of X_t, small μ, and small M_A, which can be probed at the Tevatron, we need the sign of μA_t to be negative so that the stop-chargino contribution to $b \to s\gamma$ amplitude in Eq. (33) cancels against that of the charged Higgs in Eq. (32) [21]. The $B_s \to \mu^+\mu^-$ constraint in this scenario is quite strong because the $B_s \to \mu^+\mu^-$ branching ratio in Eq. (14) is proportional to A_t, which is large, and in the denominator the factor $1 + \epsilon_3 \tan\beta \sim 1$, as the ϵ_3 loop factor is small. The $B_u \to \tau\nu$ constraint has two allowed regions related to the two possible signs of the amplitude, as can be seen in Eq. (39). At low values of $\tan\beta$ and large values of M_A the SM contribution dominates, while at complementary values of M_A and $\tan\beta$ the SUSY contribution dominates.

In Fig. 2(a) the present limit on the $B_s \to \mu^+\mu^-$, and the measurements of the $b \to s\gamma$ and $B_u \to \tau\nu$ decay rates

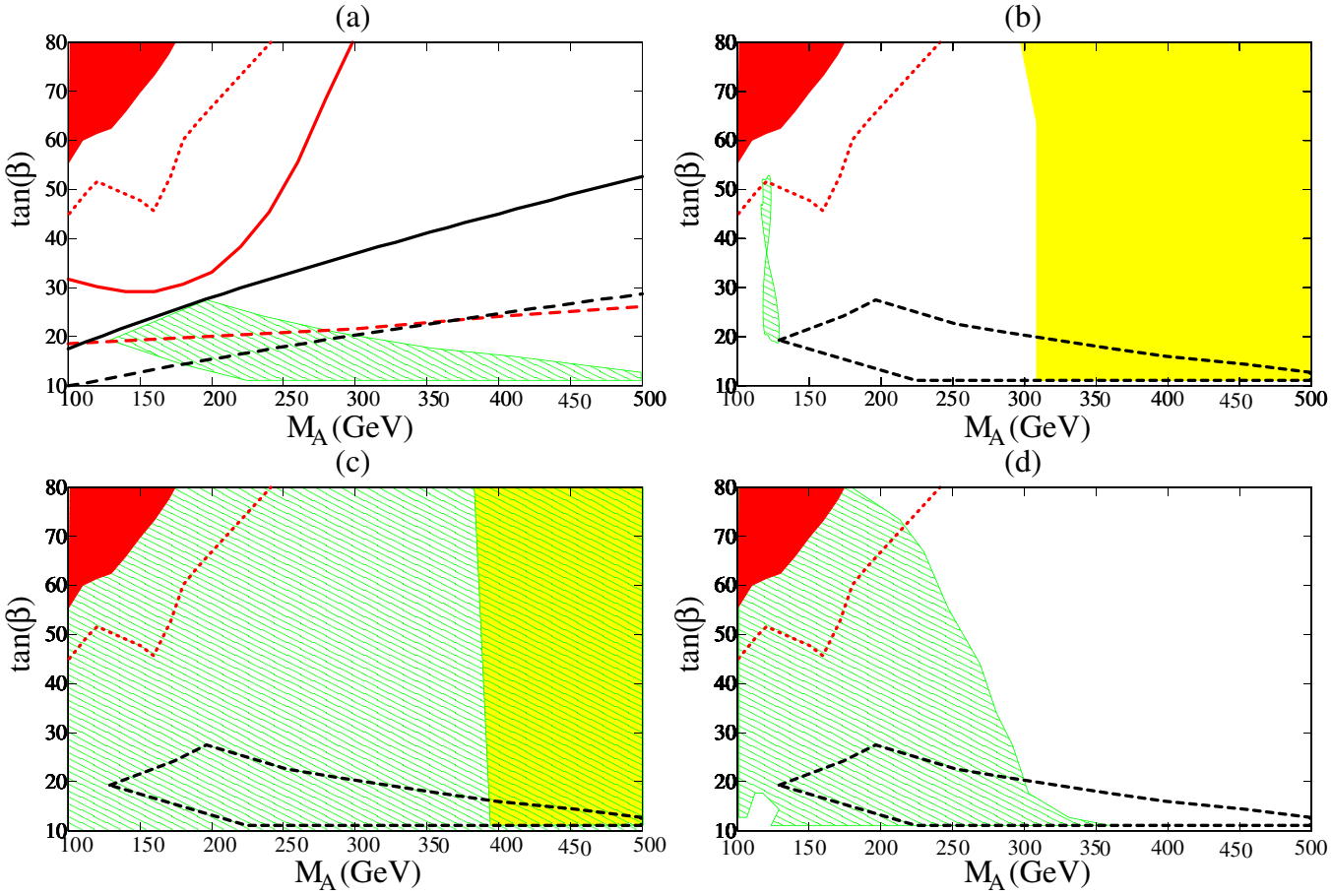

FIG. 2 (color online). The gray (red) region, in all four figures, is excluded by the CDF experiment's search for nonstandard Higgs bosons in the inclusive $A \to \tau^+\tau^-$ channel at 1 fb^{-1} luminosity. The dotted line shows the corresponding D0 excluded region at 1 fb^{-1}. (a) The solid and dashed lines represent the future reach for the Tevatron (at 4 fb^{-1}) and LHC (at 10 fb^{-1} for $B_s \to \mu^+\mu^-$ and at 30 fb^{-1} for $A \to \tau^+\tau^-$), respectively, where the dark gray (red) lines correspond to the nonstandard Higgs search reaches in the $H \to \tau\tau$ channel while the black lines are the projected $\mathcal{BR}(B_s \to \mu^+\mu^-)$ bounds for $\mu = -100$ GeV, $X_t = 2.4$ TeV, $M_{\rm SUSY} = 1$ TeV, and $M_3 = 0.8$ TeV. The gray (green) hatched regions are those allowed by the present B-physics constraints on the $B_u \to \tau\nu$ $b \to s\gamma$ and $B_s \to \mu^+\mu^-$ branching ratios. (b) and (c) For the same SUSY mass parameters the light gray (yellow) area is the 5σ discovery region in the $h \to \gamma\gamma$ channel, while the gray (green) hatched area is the same for the $h \to \tau\tau$ channel for the CMS and ATLAS experiments, respectively, at 30 fb^{-1}. (d) the gray (green) hatched region is the 3σ evidence region for the SM-like Higgs searches (at 4 fb^{-1}) at the Tevatron. (b)–(d) The areas surrounded by the dashed black curves correspond to the regions allowed by present B-physics constraints.

allow the gray (green) hatched region for $X_t = 2.4$ TeV, $M_3 = -800$ GeV, $M_{\rm SUSY} = 1$ TeV, and $\mu = -100$ GeV. The dark gray (red) region is excluded by the CDF experiment's nonstandard Higgs search in the inclusive $\tau^+\tau^-$ decay mode. The dark gray (red) dotted curve is the corresponding excluded region according to the D0 collaboration. The dark gray (red) solid and dashed curves show the regions that can be excluded by nonstandard Higgs searches at the Tevatron for a future luminosity of 4 fb^{-1} and at the LHC for a luminosity of 30 fb^{-1}, respectively. The black solid and dashed curves correspond to the future $B_s \to \mu^+\mu^-$ limits for the Tevatron at a luminosity of 4 fb^{-1} and the LHC at a luminosity of 10 fb^{-1} shown in Eqs. (20) and (21), respectively. A reach similar to Eq. (21) and comparable to the standard model prediction is expected at LHCb with only a few fb^{-1} of data [36]. As the B-physics allowed region corresponds to large values of M_A and small values of $\tan\beta$, the SM contribution to the amplitude of the $B_u \to \tau\nu$ process is larger than the SUSY contribution to the same amplitude. The region where the SUSY contribution to the amplitude of the $B_u \to \tau\nu$ process is larger than the SM contribution is excluded by the present bounds on the $B_s \to \mu^+\mu^-$ branching ratio in Eq. (19).

As we found in Ref. [21] the maximal mixing scenario is strongly constrained by B physics and the addition of the $B_u \to \tau\nu$ limit makes these constraints even stronger. For these values of SUSY parameters B-physics constraints prefer low to moderate values of $\tan\beta$. In addition the Tevatron will find it difficult to discover a nonstandard Higgs boson for this scenario. Moreover, the LHC at a luminosity of 30 fb^{-1} will only be able to probe a very small portion of the B-physics allowed parameter space in the $A/H \to \tau\tau$ channel.

In Figs. 2(b) and 2(c) we show the parts of the M_A-$\tan\beta$ that can be probed in standard model Higgs searches at the CMS and ATLAS experiments, respectively. The light gray (yellow) regions are those that can be probed in the $h \to \gamma\gamma$ channel while the dark gray (green) hatched regions can be probed in the $h \to \tau\tau$ channel with a luminosity of 30 fb^{-1} at 5σ. Present available studies with the ATLAS detector show that it will be able to probe all of the B-physics allowed region. According to the new analysis shown in Ref. [28], the CMS detector may not be able to probe the region of moderate M_A in the $h \to \tau\tau$ channel. However due to a significant improvement in the CMS sensitivity in the $\gamma\gamma$ channel a large portion of the B-physics allowed region can still be probed. If the sign of $A_t M_3$ were positive the qualitative features of the CMS reach and ATLAS reach would remain the same.

In Fig. 2(d) we show the region of the M_A-$\tan\beta$ plane that the Tevatron can probe in the $h \to b\bar{b}$ channel with a luminosity of 4 fb^{-1} per experiment and a signal significance of 3 standard deviations. For the modified maximal mixing scenario the region that can be probed is relatively large compared to the standard one [24,32], because the sign of $A_t M_3$ is negative. For negative $A_t M_3$ the maximum SM-like Higgs boson mass is approximately $\sim$125 GeV compared to the standard maximal mixing scenario which has 130 GeV as the maximum Higgs mass [49].

In Fig. 3 we show the effect of going to a lower value of stop mixing parameter $X_t = 1$ TeV. There are two disconnected B-physics allowed regions for these SUSY parameters shown in Fig. 3(a). There is a tiny upper region at around $(M_A, \tan\beta) \sim (150\ \text{GeV}, 43)$ and a much larger lower $\tan\beta$ region where all the B-physics constraints are just satisfied. In the upper region the SUSY contribution to the amplitude of the $B_u \to \tau\nu$ rate is larger than the SM contribution to the same process, while in the lower region the opposite is true. The area between these two regions is excluded because the ratio $R_{B\tau\nu}$ in Eq. (40) is below the 2σ bound. The reach via SM-like Higgs searches for these SUSY parameters are similar to the maximal mixing scenario. CMS has difficulties seeing the SM-like Higgs in part of the regions allowed by B-physics constraints, but the ATLAS experiment will cover all of the M_A-$\tan\beta$ plane. The Tevatron experiments may now cover the whole allowed region of the M_A-$\tan\beta$ plane at 3σ.

B. Large μ and small or negligible X_t

For the minimal mixing scenario, X_t is equal to zero and the chargino-stop contribution to the $b \to s\gamma$ process is small. Because of a reasonable agreement between the standard model prediction and the experimental measurement of the $b \to s\gamma$ rate, we need the charged Higgs contribution in Eq. (32) to be small. For a light charged Higgs, this requirement can be achieved by going to large values of μ, M_3, and $\tan\beta$ because of a cancellation between the tree-level term and the loop induced term in Eq. (32). Since A_t is small, the $B_s \to \mu^+\mu^-$ limit puts a weak constraint on the M_A-$\tan\beta$ plane. Additionally, for these values of parameters the usual bound on $\tan\beta$ that comes from requiring that y_b be perturbative up to the grand unified theory (GUT) scale may be relaxed: Since the bottom Yukawa has the form

$$y_b \simeq \frac{\sqrt{2} m_b \tan\beta}{v(1 + \epsilon_3 \tan\beta)} \tag{42}$$

and as $\epsilon_3 \tan\beta$ needs to be real, positive, and of order one, for the above cancellation in the charged Higgs amplitude to occur,[2] the denominator suppresses the bottom Yukawa coupling for large values of $\tan\beta$.

The SM-like Higgs searches put an interesting constraint on scenarios with large values of $|\mu|$ and small values of X_t, since unless $M_{\rm SUSY}$ is sufficiently large the SM-like Higgs mass tends to be below the LEP bound of 114.4 GeV.

[2]An exact cancellation is not needed due to the theoretical and experimental uncertainties so a small phase is also allowed.

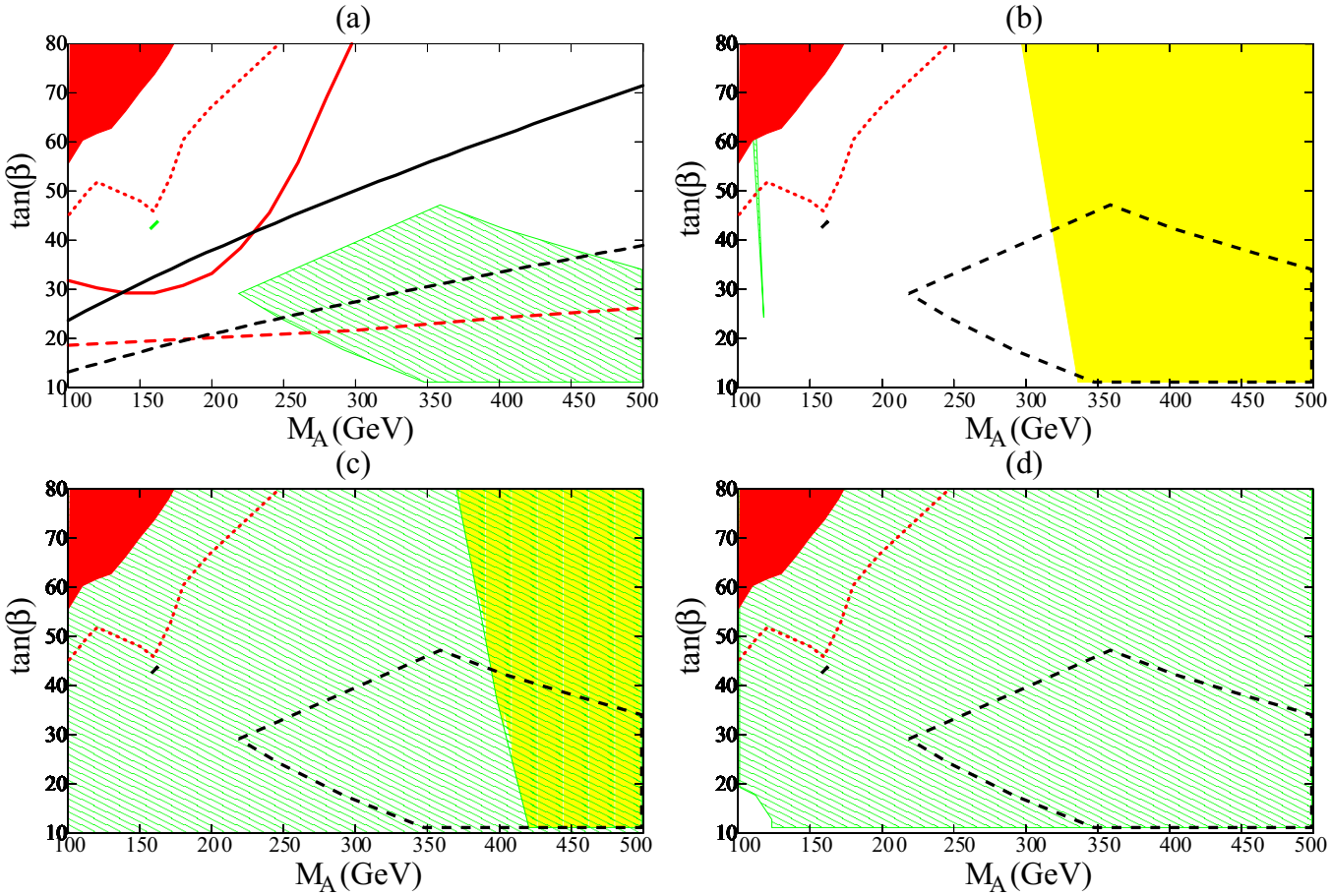

FIG. 3 (color online). (a)–(d) The lines and the colors correspond to the same quantities as in Fig. 2, where the SUSY parameters are the same except for $X_t = 1$ TeV.

The impact of the LEP bound on the excluded region in the M_A-tanβ plane is very sensitive to μ, $M_{\rm SUSY}$, and the top mass. For instance, for $M_{\rm SUSY} \sim 1$ TeV this scenario is highly constrained by the LEP bounds on the SM-like Higgs mass, but increasing $M_{\rm SUSY}$ to 2 TeV is sufficient to avoid this constraint [56].

The corresponding results for $M_{\rm SUSY} = 2$ TeV are shown in Fig. 4. We have previously analyzed this scenario in Ref. [21] without adding the $B_u \to \tau\nu$ constraints. In Fig. 4 we see that the addition of this new constraint excludes the diagonal region with corners (100 GeV, 38), (155 GeV, 28), (450 GeV, 80), and (190 GeV, 65) for the parameters $\mu = 1.5 M_{\rm SUSY}$ and $M_3 = 0.8 M_{\rm SUSY}$. In Fig. 4(a) we show the effect of the LEP bound on the B-physics allowed regions. The region below the black (blue) solid line shows the area excluded by the LEP bound in the M_A-tanβ plane.

From Figs. 4(b) and 4(c) it is clear that the CMS and ATLAS experiment can probe most of the allowed B-physics regions of the M_A-tanβ plane, using SM-like Higgs searches in the $h \to \gamma\gamma$ and the $h \to \tau\tau$ channels. CMS has an inaccessible region at large M_A in the $\tau\tau$-channel because in this region the τ Yukawa coupling is only slightly above the standard model value and according to Ref. [28] CMS does not have a 5σ signal significance with 30 fb^{-1} of data for any standard model Higgs mass. However, given that the Higgs mass and the $h \to \tau\tau$ coupling vary smoothly with M_A and tanβ the discovery potential is also above 4σ for most of the region that appears inaccessible in Fig. 4(b). Again, at 4 fb^{-1} the Tevatron could have a 3σ evidence over most of the parameter space allowed by B-physics and the LEP Higgs mass bound.

We would like to stress that the B-physics and the LEP excluded regions, for the minimal mixing scenario, allow a clear region of $M_A = 130$–170 GeV and tan$\beta = 50$–70. These values are easily within the Tevatron's sensitivity region for nonstandard Higgs searches in the $\tau\tau$ channel. In addition, the SM-like Higgs boson mass is close to the current limit and therefore should be visible at the Tevatron at the 3σ level with an increase in sensitivity and luminosity. Both CDF and D0 collaborations have recently made public their findings in the inclusive $A \to \tau\tau$ channel at a luminosity of 1 fb^{-1}. The CDF experiment finds a slight excess [26] while the D0 experiment [25] finds a reduction in the signal for the same values of the $\tau\tau$ visible mass. The

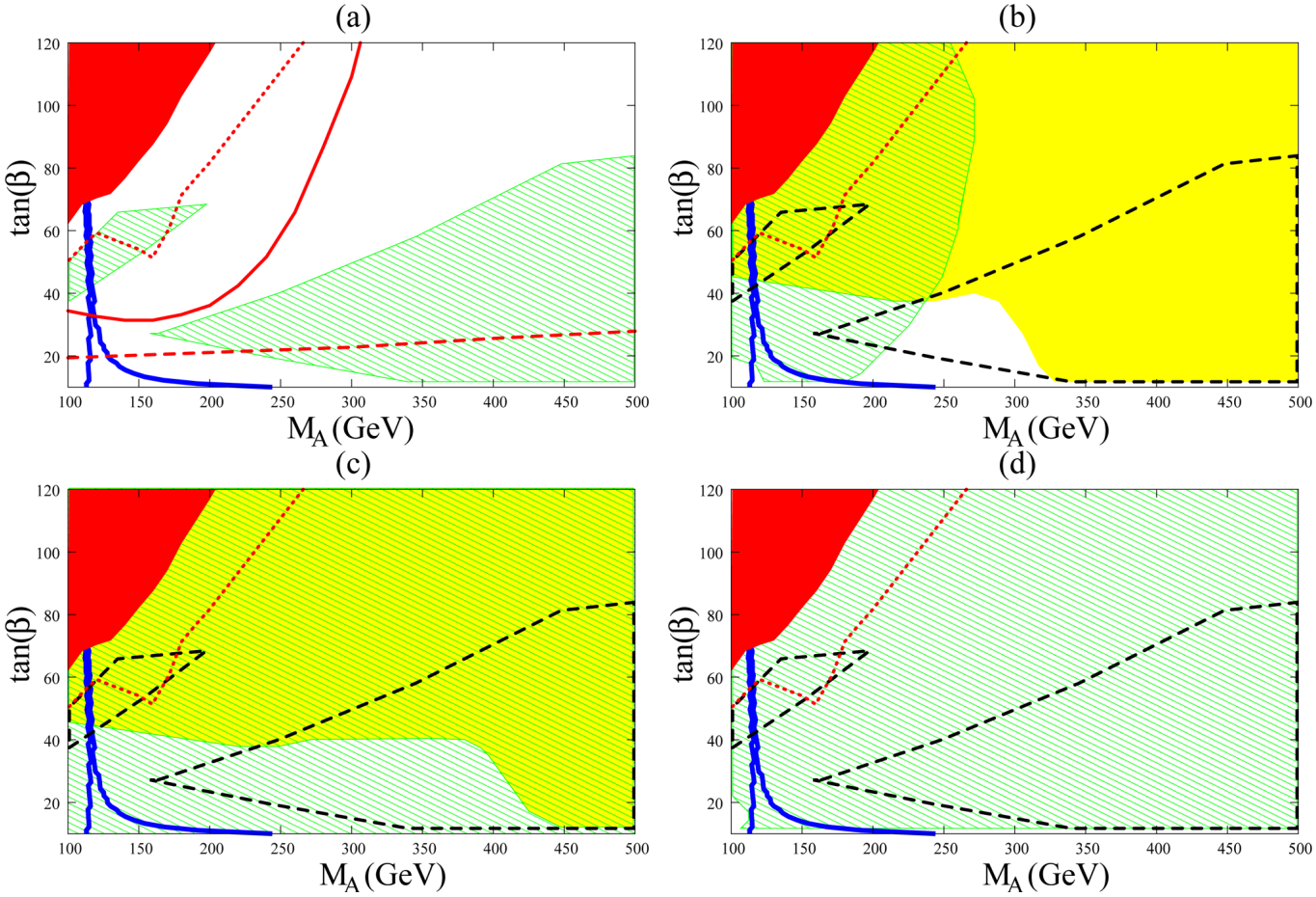

FIG. 4 (color online). (a)–(d) The lines and the colors correspond to the same quantities as in Fig. 2, where the SUSY parameters are the same except for $X_t = 0$ GeV, $\mu = 1.5 M_{\rm SUSY}$, and $M_{\rm SUSY} = 2$ TeV. The region below the black (blue) solid line corresponds to the area excluded by the LEP bound on the SM-like Higgs boson for $m_t = 170.9$ GeV.

D0 limit further limits the upper B-physics allowed region to values of $M_A = 130$–150 GeV and $\tan\beta \sim 55$.

This scenario can be relatively insensitive to small changes in the value of X_t. It would seem that increasing the value of X_t would make the $B_s \to \mu^+\mu^-$ constraint extremely strong. However, there is a $1/\mu^2$ dependence from the $(1+\epsilon_0^3)(1+\epsilon_3)$ factor in the denominator of Eq. (14) and only a linear μ dependence in its numerator. Thus as long as the loop factors ϵ are positive and μ is large, even moderate values of X_t do not strengthen the $B_s \to \mu^+\mu^-$ constraint. Additionally at large values of μ, M_3, and $\tan\beta$ the charged Higgs contribution to the $b \to s\gamma$ amplitude in Eq. (32) may have the opposite sign to the SM one, a novel result that only occurs for this range of parameters. In this region of parameter space, to cancel this negative charged Higgs amplitude we need the chargino-stop contribution in Eq. (33) to be positive or the sign of μA_t to be positive.

C. Small $\alpha_{\rm eff}$

This scenario was studied in Ref. [56] in which the off-diagonal components of the CP-even Higgs mass matrix are approximately zero. This approximate cancellation can be achieved by making, for instance, the following choice of parameters

$$\mu = 2.5 \text{ TeV}, \qquad X_t = -1200.0 \text{ TeV}, \qquad M_{\rm SUSY} = 800 \text{ GeV}, \qquad M_3 = 500 \text{ GeV}. \tag{43}$$

A consequence of this cancellation is that the couplings of the SM-like Higgs boson to the b quarks and τ leptons are suppressed.

In Fig. 5 we present the effect of this choice of parameters on the B-physics allowed region and on Higgs searches at the LHC and Tevatron. The B-physics constraints are quite severe and similar to the large X_t scenario we discussed above. The $h \to \gamma\gamma$ channel for SM-like Higgs searches is enhanced because the $h \to \tau\bar{\tau}$ and $h \to b\bar{b}$ branching ratios are suppressed, leading to an enhancement of the $h \to \gamma\gamma$ branching ratio. Therefore the CMS and ALTAS experiments will be able to probe a large part of the M_A-$\tan\beta$ plane in the $h \to \gamma\gamma$ channel. The Tevatron will not be able to probe most of the B-physics allowed region because of the suppression of the $h \to b\bar{b}$ branching ratio.

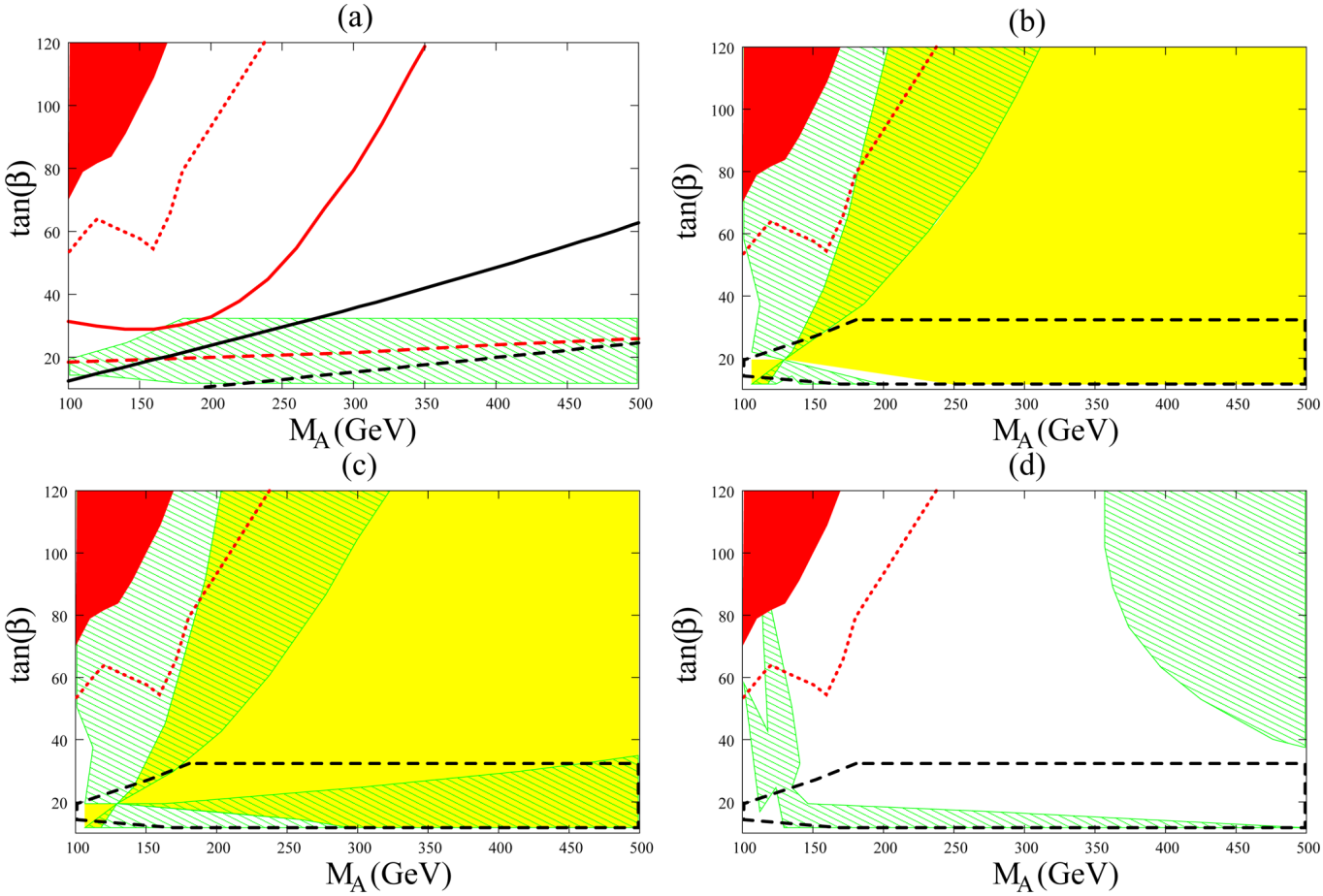

FIG. 5 (color online). (a)–(d) The lines and the colors correspond to the same quantities as in Fig. 2, where the SUSY parameters are the same except for $M_3 = 500$ GeV, $M_{\rm SUSY} = 800$ GeV, $X_t = -1.2$ TeV, and $\mu = 2.5$ TeV.

IV. CONCLUSIONS

In this article we have studied the interplay between B-physics constraints and Higgs searches at hadron colliders in the framework of minimal flavor violating SUSY models. The results we present here depend on the projected sensitivities of the CMS and ATLAS experiments and the Tevatron collider in the different SM-like and nonstandard Higgs boson channels. The Tevatron projections assumed in this work [55] need to be further solidified by improvements in the analyses that CDF and D0 are performing. Both CMS and ATLAS have recently performed improvements in their projections in the $\gamma\gamma$ inclusive channel and CMS has also recently updated their $h \to \tau\tau$ vector boson fusion study [28]. We have illustrated this interplay between Higgs searches at hadron colliders and B-physics constraints using four benchmark scenarios.

In particular the B-physics constraints are extremely severe for SUSY parameters which have large values of X_t and small values of μ. For SM-like Higgs boson searches the LHC experiments should be able to probe all of the allowed region of parameter space with 30 fb^{-1}, but the Tevatron collider will have difficulties doing this with 4 fb^{-1} of data. Discovering a SM-like Higgs boson at the CMS experiment with 30 fb^{-1} of data will be challenging in this scenario, since CMS has a better sensitivity in the $h \to \gamma\gamma$ rather than in the $h \to \tau\tau$ channel and as the $hb\bar{b}$ and the $h\tau\bar{\tau}$ couplings are somewhat enhanced for moderate or small M_A, the $h \to \gamma\gamma$ branching ratio is smaller than in the SM. On the other hand, the ATLAS experiment will easily probe the allowed region of parameter space because the $h \to \tau\tau$ branching ratio is enhanced for these values of SUSY parameters. The Tevatron will find it very difficult to detect a SM-like Higgs in this scenario because the SM-like Higgs is heavy and the signal significance, in the $h \to b\bar{b}$ channel, drops sharply with increasing Higgs mass. Additionally, in this scenario the B-physics constraints favor regions which have large values of M_A and low values of tanβ while the nonstandard Higgs boson searches at hadron colliders are less efficient in these regions. Therefore at a luminosity of 30 fb^{-1} the LHC will be able to observe the SM-like Higgs, but may find it difficult to discover nonstandard Higgs bosons.

The B-physics constraints are far weaker for large values of μ and small values of X_t due to a suppression of SUSY

contributions to the $B_s \to \mu^+\mu-$ and the $b \to s\gamma$ rates. At the same time the present LEP bounds on the SM-like Higgs mass put strong constraints on the allowed regions of parameter space, in particular for $M_{\rm SUSY} \leq 1$ TeV. For the minimal mixing scenario with $M_{\rm SUSY} = 2$ TeV we have studied, the LHC will be able to probe most of the B-physics allowed region in nonstandard Higgs searches, for values of $M_A < 500$ GeV. For SM-like Higgs searches, with 30 fb^{-1} of data, the CMS collaboration should be able to probe most of the allowed regions, while the ATLAS collaboration will be able to probe all of them. In addition, this scenario is the most promising for the Tevatron to detect both the SM-like Higgs and the nonstandard Higgs bosons in the near future.

The final benchmark scenario we studied was that of small $\alpha_{\rm eff}$. Because of the suppression of SM-like Higgs couplings to b quarks and τ's, the $\gamma\gamma$ channel is enhanced. Because of this enhancement both the LHC experiments will be able to discover the SM-like Higgs over most of the B-physics allowed parameter space. The Tevatron will find it difficult to detect a SM-like Higgs due to its mass and suppressed couplings to $b\bar{b}$.

In conclusion, scenarios with lower values of stop mixing parameter X_t and larger values of Higgsino mass parameter μ will be easier to probe at hadron colliders through direct Higgs searches of both standard and nonstandard Higgs bosons. At larger values of X_t, direct nonstandard Higgs boson searches are strongly constrained by present bounds on B-physics observables. On the other hand, the SM-like Higgs boson mass is enhanced through radiative corrections, rendering it more easily detectable at the LHC. Finally, the observation of a SM-like Higgs in the $h \to \tau\tau$ channel and not in the $h \to \gamma\gamma$ or vice versa, may be used to obtain additional information on the values of the supersymmetry breaking parameters.

ACKNOWLEDGMENTS

M. C. and C. W. would like to thank the Aspen Center for Physics, where part of this work was done. We wish to thank Patricia Ball, Thomas Becher, Avto Kharchilava, Enrico Lunghi, and Matthias Nuebert. Work at ANL is supported in part by the U.S. DOE, Division of HEP, Contract No. DE-AC02-06CH11357. Fermilab is operated by Universities Research Association Inc. under Contract No. DE-AC02-76CH02000 with the DOE. This work was also supported in part by the U.S. Department of Energy through Grant No. DE-FG02-90ER40560. This work was also partially supported by the University of Chicago under section H.28 of its Contract No. W-31-109-ENG-38 to manage Argonne National Laboratory.

[1] J. R. Ellis, G. Ridolfi, and F. Zwirner, Phys. Lett. B **257**, 83 (1991); **262**, 477 (1991); Y. Okada, M. Yamaguchi, and T. Yanagida, Prog. Theor. Phys. **85**, 1 (1991); M. A. Diaz and H. E. Haber, Phys. Rev. D **45**, 4246 (1992).
[2] M. Carena, J. Espinosa, M. Quirós, and C. Wagner, Phys. Lett. B **355**, 209 (1995); M. Carena, M. Quirós, and C. Wagner, Nucl. Phys. **B461**, 407 (1996).
[3] M. Carena, M. Quiros, and C. E. M. Wagner, Nucl. Phys. **B461**, 407 (1996).
[4] H. E. Haber, R. Hempfling, and A. H. Hoang, Z. Phys. C **75**, 539 (1997).
[5] S. Heinemeyer, W. Hollik, and G. Weiglein, Eur. Phys. J. C **9**, 343 (1999).
[6] M. Carena, H. Haber, S. Heinemeyer, W. Hollik, C. Wagner, and G. Weiglein, Nucl. Phys. **B580**, 29 (2000); J. R. Espinosa and R. J. Zhang, J. High Energy Phys. 03 (2000) 026.
[7] J. Espinosa and R. Zhang, Nucl. Phys. **B586**, 3 (2000).
[8] A. Brignole, G. Degrassi, P. Slavich, and F. Zwirner, Nucl. Phys. **B631**, 195 (2002); **B643**, 79 (2002).
[9] G. Degrassi, S. Heinemeyer, W. Hollik, P. Slavich, and G. Weiglein, Eur. Phys. J. C **28**, 133 (2003).
[10] M. Carena and H. E. Haber, Prog. Part. Nucl. Phys. **50**, 63 (2003).
[11] S. Heinemeyer, W. Hollik, H. Rzehak, and G. Weiglein, Eur. Phys. J. C **39**, 465 (2005).
[12] S. Martin, Phys. Rev. D **67**, 095012 (2003); **71**, 016012 (2005).
[13] S. Bertolini, F. Borzumati, A. Masiero, and G. Ridolfi, Nucl. Phys. **B353**, 591 (1991).
[14] G. Isidori and A. Retico, J. High Energy Phys. 11 (2001) 001.
[15] A. J. Buras, P. H. Chankowski, J. Rosiek, and L. Slawianowska, Phys. Lett. B **546**, 96 (2002).
[16] A. J. Buras, P. H. Chankowski, J. Rosiek, and L. Slawianowska, Nucl. Phys. **B659**, 3 (2003).
[17] K. S. Babu and C. F. Kolda, Phys. Rev. Lett. **84**, 228 (2000).
[18] A. Dedes and A. Pilaftsis, Phys. Rev. D **67**, 015012 (2003).
[19] D. A. Demir, Phys. Lett. B **571**, 193 (2003).
[20] J. Foster, K. i. Okumura, and L. Roszkowski, J. High Energy Phys. 08 (2005) 094.
[21] M. Carena, A. Menon, R. Noriega-Papaqui, A. Szynkman, and C. E. M. Wagner, Phys. Rev. D **74**, 015009 (2006).
[22] K. Ikado *et al.*, Phys. Rev. Lett. **97**, 251802 (2006).
[23] B. Aubert *et al.* (*BABAR* Collaboration), arXiv:hep-ex/0608019.
[24] M. Carena, S. Heinemeyer, C. E. M. Wagner, and G. Weiglein, Eur. Phys. J. C **45**, 797 (2006).
[25] http://www-d0.fnal.gov/Run2Physics/WWW/results/prelim/HIGGS/H29/ D0 Note 5331-CONF.
[26] http://www.physics.ucdavis.edu/%7Econway/talks/ConwayAspen2007.pdf.
[27] See, for example, B. Heinemann presentation to the P5

Committee, Fermilab, September 2006, http://hep.ph.liv.ac.uk/beate/homepage/p5-discovery.pdf.

[28] A. Nikitenko, ICHEP Conference 2006, Moscow, Russia, 2006, http://ichep06.jinr.ru/reports/327_7s6_17p10_nikitenko.ppt; ATLAS note SN-ATLAS-2003-024; F. Gianotti, in Proceedings of the ICHEP Conference 2006, Moscow, Russia, 2006 (unpublished), http://ichep06.jinr.ru/programme.asp; http://documents.cern.ch/cgi-bin/setlink?base=atlnot&categ=CONF&id=phys-conf-2006-018.

[29] M. Carena, D. Hooper, and P. Skands, Phys. Rev. Lett. **97**, 051801 (2006); M. Carena, D. Hooper, and A. Vallinotto, Phys. Rev. D **75**, 055010 (2007).

[30] M. Carena, S. Mrenna, and C. E. M. Wagner, Phys. Rev. D **60**, 075010 (1999); **62**, 055008 (2000).

[31] L. Roszkowski, R. R. de Austri, and R. Trotta, J. High Energy Phys. 04 (2007) 084.

[32] U. Aglietti *et al.*, arXiv:hep-ph/0612172.

[33] G. Buchalla, A. J. Buras, and M. E. Lautenbacher, Rev. Mod. Phys. **68**, 1125 (1996).

[34] R. Bernhard *et al.* (CDF Collaboration), arXiv:hep-ex/0508058.

[35] Nikolai Nikitine, Opening plenary meeting: ''Flavor in the era of the LHC'' CERN, 2005; R. McPherson, in Proceedings of the Aspen Winter Conference, Aspen, CO, 2006 (unpublished), http://www.aspenphys.org.

[36] http://teubert.web.cern.ch/teubert/BsmumuLHCb.ppt.

[37] M. Bona *et al.* (UTfit Collaboration), J. High Energy Phys. 10 (2006) 081.

[38] J. Charles *et al.* (CKMfitter Group), Eur. Phys. J. C **41**, 1 (2005); http://www.slac.standford.edu/xorg/ckmfitter/plots_eps2005/ckmEval_results_eps_05.ps.

[39] V. M. Abazov *et al.* (D0 Collaboration), Phys. Rev. Lett. **97**, 021802 (2006).

[40] S. Giagu (CDF Collaboration), arXiv:hep-ex/0610044.

[41] Heavy Flavor Averaging Group (HFAG), arXiv:hep-ex/0603003.

[42] T. Becher and M. Neubert, Phys. Rev. Lett. **98**, 022003 (2007).

[43] G. Degrassi, P. Gambino, and G. F. Giudice, J. High Energy Phys. 12 (2000) 009.

[44] M. Carena, D. Garcia, U. Nierste, and C. E. M. Wagner, Phys. Lett. B **499**, 141 (2001).

[45] G. Isidori and P. Paradisi, Phys. Lett. B **639**, 499 (2006).

[46] W. S. Hou, Phys. Rev. D **48**, 2342 (1993).

[47] A. G. Akeroyd and S. Recksiegel, J. Phys. G **29**, 2311 (2003).

[48] E. Brubaker *et al.* (Tevatron Electroweak Working Group), arXiv:hep-ex/0608032.

[49] J. S. Lee, A. Pilaftsis, M. Carena, S. Y. Choi, M. Drees, J. R. Ellis, and C. E. M. Wagner, Comput. Phys. Commun. **156**, 283 (2004).

[50] S. Abdullin *et al.*, Eur. Phys. J. C **39S2**, 41 (2005).

[51] R. Kinnunen and S. Lehti, CMS Note 2006/075.

[52] A. Kalinowski, M. Konecki, and D. Kotlinski, CMS Note 2006/105.

[53] S. Lehti, CMS Note 2006/101.

[54] S. Gennai, S. Heinemeyer, A. Kalinowski, R. Kinnunen, S. Lethi, A. Nikitenko, and G. Weiglein, arXiv:0704.0619v1.

[55] L. Babukhadia *et al.* (CDF and D0 Working Group Members), FERMILAB-PUB-03-320-E.

[56] M. Carena, S. Heinemeyer, C. E. M. Wagner, and G. Weiglein, Eur. Phys. J. C **26**, 601 (2003).